

Time-resolved surface charge change on the cytoplasmic side of bacteriorhodopsin

U. Alexiev^{a,*}, P. Scherrer^{a,**}, T. Marti^{b,***}, H.G. Khorana^b, M.P. Heyn^a

^aBiophysics Group, Freie Universität Berlin, Arnimallee 14, D-14195 Berlin, Germany

^bDepartment of Biology and Chemistry, MIT, Cambridge, MA 02139, USA

Received 5 July 1995; revised version received 13 August 1995

Abstract The pH-sensitive dye 5-iodoacetamidofluorescein was covalently bound to a single cysteine residue introduced by site-directed mutagenesis in position 101 on the cytoplasmic surface or in position 130 on the extracellular surface of the proton pump bacteriorhodopsin. Using time-resolved absorption spectroscopy at 495 nm a transient increase was observed in the apparent pK of the dye attached at residue 101. At pH 7.3 the rise and decay times of this pK-change (~2 ms and ~60 ms) correlate well with decay times observed for the M and O intermediates and with the proton uptake time. Interpreting the pK-increase of +0.18 pH-unit in terms of a transiently more negative surface charge density, we calculate a change of -0.80 elementary charge per bacteriorhodopsin at the cytoplasmic surface. It is likely that this charge change is due to the transient deprotonation of aspartate-96. With the label in position 130 on the extracellular surface no transient pK-shift was detected.

Key words: Surface charge density; Gouy-Chapman theory; Transient surface potential changes; Bacteriorhodopsin; Photocycle

1. Introduction

We have detected transient changes in the apparent pK of a surface bound pH-indicator during the photocycle of the light-driven proton pump bacteriorhodopsin (bR). Upon light excitation, bR undergoes a photocycle with several intermediates (J, K, L, M, N and O) which is accompanied by the net transport of one proton from the cytoplasmic to the extracellular side of the purple membrane. In the first half of the photocycle, the Schiff base proton is transferred to aspartate-85 [1], and a proton is released to the extracellular medium. In the second half of the photocycle the Schiff base is reprotonated

during the M-to-N transition from aspartate-96 [2,3]. Aspartate-96 is reprotonated from the cytoplasmic side in the N-to-O transition. Recently we determined the surface charge density and the light-induced proton release kinetics of bR reconstituted in micelles using the pH-indicator dye fluorescein covalently bound to various positions on the extracellular and cytoplasmic surface [4–6]. Selective labeling was achieved by using bR mutants with a single cysteine residue in the surface loops [4–6]. The Gouy-Chapman theory was tested and shown to be applicable and valid to determine the surface charge density of bR monomers [4]. A uniform charge density was detected on both surfaces, with the cytoplasmic side being more negatively charged than the extracellular surface (-2.6 and -1.8 elementary charges per bR, respectively [4]). In this study we monitor the light induced changes in the apparent pK (pK_{app}) of the surface bound pH-indicator during the photocycle. The pK_{app} -changes are interpreted in terms of transient changes in the surface charge occurring during the proton uptake process. Various methods have been used in the past to measure transient surface potential changes in bR [7–10]. Our approach has the advantage that with labels at selected and well defined positions we can distinguish between contributions from either side of the protein and that we correlate the kinetics of the transient charge changes with that of the photocycle and of the proton uptake from the bulk medium.

2. Materials and methods

1,2-Dimyristoyl-*sn*-glycero-3-phosphatidylcholine (DMPC), 3-[(3-cholamidopropyl)dimethylammonio]-1-propanesulfonate (CHAPS), 4-morpholinepropanesulfonate (MOPS), 2-morpholinoethanesulfonate (MES), and tris(hydroxymethyl)-aminomethane (Tris) were obtained from Sigma. 5-(Iodoacetamido)-fluorescein was from Molecular Probes.

The construction of genes coding for the single mutants containing a unique cysteine residue, their expression in *Escherichia coli*, and the purification of the bacterioopsin apoprotein have been described [11].

Renaturation of freeze-dried bO mutant protein in DMPC/CHAPS micelles, labeling with 5-(iodoacetamido)fluorescein and the determination of the labeling stoichiometry (mol fluorescein per mol bR; 0.7 for V101C-AF and 0.85 for V130C-AF) were performed as described [4,5].

Flash spectroscopy was carried out as described elsewhere [12]. The excitation was with 10-ns pulses of 3–6 mJ of energy at 590 nm. The fraction of bR cycling was 10–15%. The light-induced surface potential change detected with fluorescein was measured as the flash-induced absorbance difference at 495 nm between samples with and without bound dye in 0.1% CHAPS, 0.0025% DMPC, 150 mM KCl and a buffer mix of 10 mM MES, MOPS, Tris at 22°C.

The change in the absorbance, ΔA , of fluorescein at 495 nm was monitored as a function of pH using a Shimadzu 250 UV/VIS spectrophotometer. To obtain the apparent pK, the data were fitted with the equation:

$$\overline{\Delta A} = \overline{\Delta A}_{max} / [1 + 10^{n(pK - pH)}] \quad (1)$$

*Corresponding author. Fax: (49) (30) 838-5186.

**Present address: Liposome Research Unit, Dept. of Biochemistry, University of British Columbia, Vancouver BC V6T 1Z3, Canada.

***Present address: Bernhard Nocht Institut für Tropenmedizin, D-20359 Hamburg, Germany.

Abbreviations: bR, bacteriorhodopsin; bO, bacterioopsin; DMPC, 1,2-dimyristoyl-*sn*-glycero-3-phosphatidylcholine; CHAPS, 3-[(3-cholamidopropyl)dimethyl-ammonio]-1-propanesulfonate; MOPS, 4-morpholinepropanesulfonate; MES, 2-morpholinoethanesulfonate; Tris, Tris(hydroxymethyl)-aminomethane; $pK_{app/in}$ and $pK_{app/tr}$, apparent pK's in the initial and transient state, respectively; pK_t , true pK; ΔpK_{tr} , transient pK-shift; V101C (or V130C), mutant with valine in position 101 (or 130) replaced by cysteine; V101C-AF (or V130C-AF), mutant V101C (or V130C) with (acetamido)fluorescein bound to cysteine.

$\overline{\Delta A}_{\max}$ is the maximal absorption difference for the alkaline form of fluorescein, n is the number of protons involved in the transition, and pK is the midpoint of the titration. From the difference between the apparent pK (pK_{app}) at a given salt concentration and the intrinsic (true) pK (pK_t), the surface potential ϕ was determined:

$$pK_t - pK_{app} = e\phi/2.3kT \quad (2)$$

The surface charge density σ was calculated from the dependence of ϕ on the salt concentration using the Gouy-Chapman equation:

$$\sinh e\phi/2kT = B\sigma C^{-1/2} \quad (3)$$

with σ expressed in electronic charge per \AA^2 and C (the concentration of KCl) in mol/liter, the value of the constant B is $134.6 (\text{mol/liter})^{1/2}$ (at 22°C and assuming a dielectric constant of 78.5).

3. Results and discussion

Measurements of the transient surface potential were performed with the pH-indicator fluorescein covalently bound to position 101 on the cytoplasmic or position 130 on the extracellular surface of bR (Fig. 1). The basis of our experiments is that a more negative surface charge leads to a more negative potential (Eqn. 3), which in turn shifts the apparent pK of the surface bound fluorescein from its initial value of $pK_{app/in}$ to a higher transient value of $pK_{app/tr} = pK_{app/in} + \Delta pK_{tr}$ (see Eqn. 2). The positive pK -shift will cause a transient decrease of the fluorescein absorbance at 495 nm. This absorbance decrease will exhibit a characteristic pH dependence (Fig. 4) given by the difference between two titration curves with slightly different pK 's, $pK_{app/in}$ and $pK_{app/tr}$. To eliminate absorbance changes as a result of transient proton concentration changes, the measurements were performed in the presence of a buffer mix containing 10 mM MES, MOPS and Tris. Since there are also absorbance changes at 495 nm due to the photocycle of bR, the

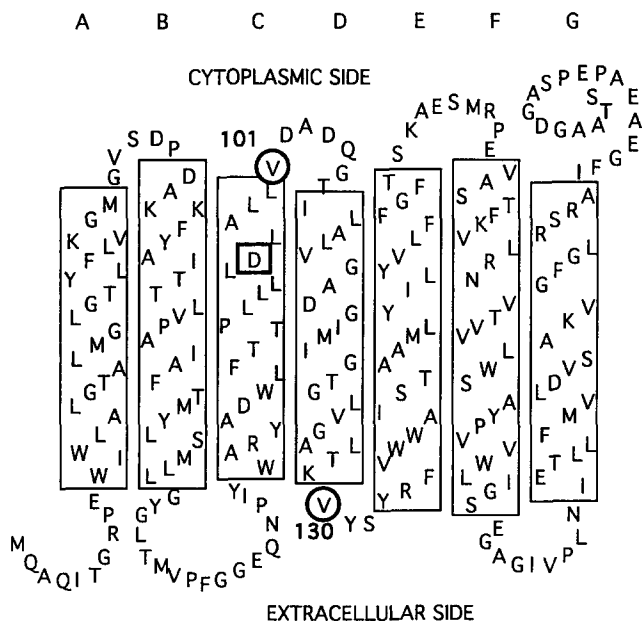


Fig. 1. Secondary structural model of bacteriorhodopsin. The seven helices labeled A-to-G are delineated by rectangles. The residues 101 and 130 changed to cysteine are circled. The residue Asp-96 is marked with a square.

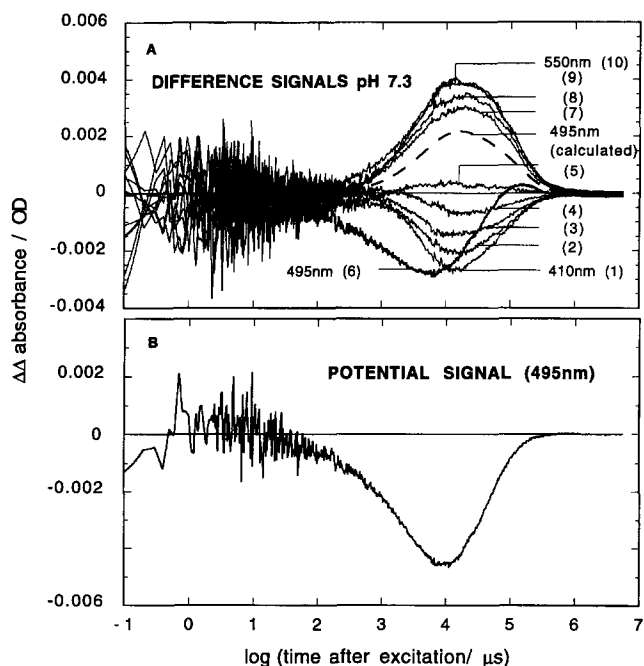


Fig. 2. (a) Differences between the transient light-induced absorbance changes at ten different wavelengths of V101C and V101C-AF in 0.1% CHAPS, 0.0025% DMPC, 150 mM KCl, and 10 mM MES, MOPS, Tris at pH 7.3 and 22°C . The trace '495nm(calculated)' (---) represents the absorption change at 495 nm due only to the difference in the photocycles of the two samples (see text). The transient absorption changes were measured in 10 nm steps from 410 to 550 nm. Ten of these are shown (1–410 nm, 2–420 nm, 3–430 nm, 4–440 nm, 5–450 nm, 6–495 nm, 7–520 nm, 8–530 nm, 9–540 nm, 10–550 nm). The logarithmic time scale is from 10^{-1} to $10^7 \mu\text{s}$. (b) Potential signal calculated as the difference between the traces labeled '495 nm' and '495nm(calculated)' of (a) (see text).

light-induced absorbance difference between samples with and without bound fluorescein was recorded. In this way the absorbance changes of the dye alone were obtained. This procedure to detect the potential signal can be used provided the photocycle kinetics in the two samples with and without dye are identical. However, Fig. 2a shows that at pH 7.3 there are small differences between the photocycle kinetics of labeled V101C-AF and unlabeled V101C at wavelengths outside the absorption band of the deprotonated dye in the time range from 100 μs to 1 s. These changes (at most 10% of the photocycle signal) are due to the labeling and were corrected for in the following way. The deprotonated form of bound fluorescein at alkaline pH absorbs between 450 and 520 nm with maximum at 495 nm. The time traces in this wavelength range (Fig. 2a) thus contain contributions from the difference in photocycle kinetics and from the absorbance changes of the dye. These differences were measured every 10 nm from 410 to 550 nm, but for clarity only the traces at 410, 420, 430, 440, 450, 495, 520, 530, 540 and 550 nm are shown in Fig. 2a. The shape of the time trace at 495 nm differs from that at the other wavelengths, since it includes the additional contribution from the potential change. Leaving out the time traces between 450 and 520 nm, the kinetics of the remaining nine absorbance differences of Fig. 2a were analyzed simultaneously with one set of time constants. This global fit required two components (4.4 ms for the rise and 132 ms for

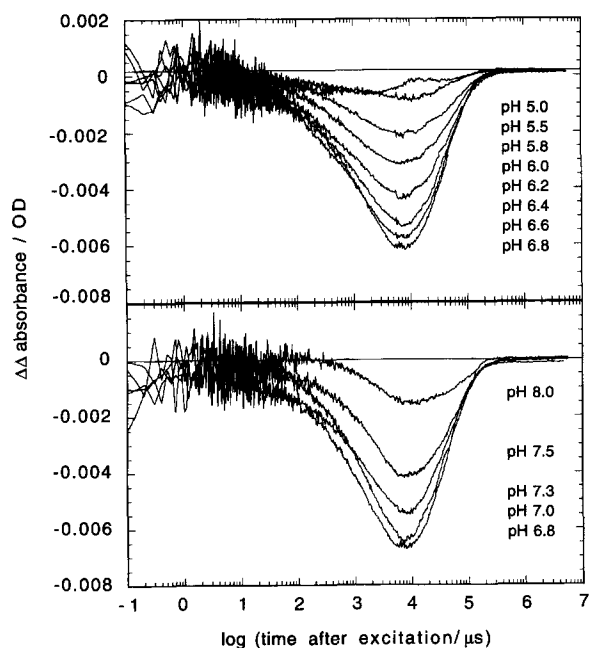


Fig. 3. Kinetics of the transient potential change at position 101 at different pH-values (5.0–8.0) obtained as in Fig. 2.

the decay). Interpolating the corresponding amplitude spectra to 495 nm, the expected time trace at 495 nm due to the photocycle difference alone was generated (trace '495 nm calculated', Fig. 2a). The simulated curve fits in well with the differences at the other wavelengths both in amplitude and times as it should be. The difference between the time traces labeled '495 nm' and '495 nm calculated' represents the time dependence of the electric potential change and is redrawn as 'potential signal' in Fig. 2b. The potential signals at 13 different pH values were obtained by the same procedure (except that only the time traces at 410, 430, 450, 530 and 550 nm were used to correct for the change in the photocycle kinetics) and are plotted in Fig. 3. The fit of the potential change with 3 exponentials for the

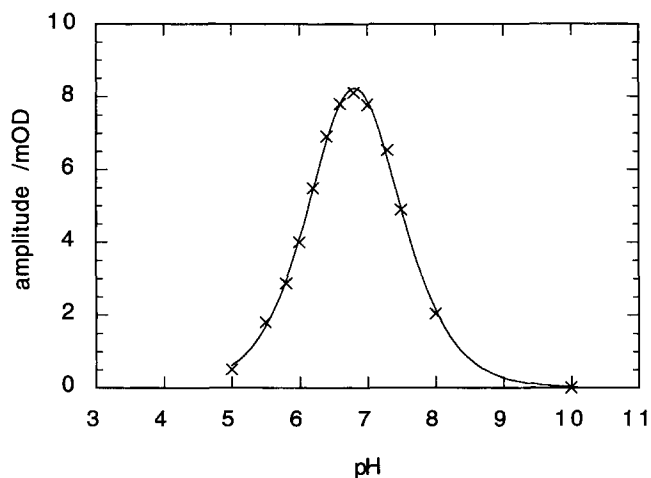


Fig. 4. pH dependence of the amplitude of the transient potential signals from Fig. 3. The continuous curve is a fit according to Eqn. 4 with $pK_{app/tr} = 6.90$ and $n = 0.95$. The errors in pH are ± 0.02 and in ΔA ± 1 –5%.

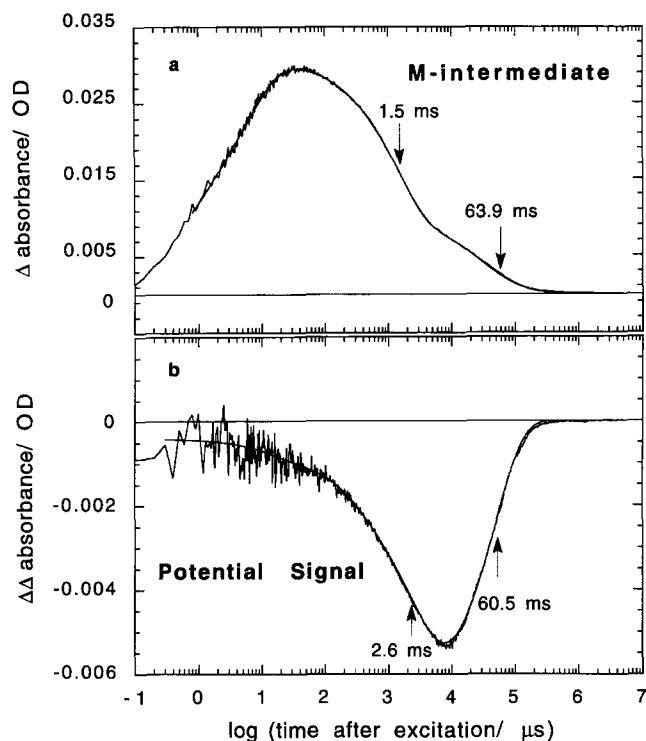


Fig. 5. Comparison of the rise and decay of the M-intermediate with the kinetics of the potential signal as detected with fluorescein bound on the cytoplasmic side in position 101. (a) Positive absorbance change ΔA at 410 nm due to the M-intermediate. (b) Negative absorbance change $\Delta\Delta A$ due to fluorescein (potential signal) at 495 nm. The vertical arrows indicate the time constants obtained from a multi-exponential fit. The conditions are 0.1% CHAPS, 0.0025% DMPC, 150 mM KCl, and 10 mM MES, MOPS, Tris at pH 7.3 and 22°C.

rise and one exponential for the decay is shown in Fig. 5. The decay amplitude is plotted as a function of pH in Fig. 4. The bell-shaped distribution of data points in Fig. 4 has the width and shape expected for the difference between two titration curves with slightly different pK 's. The data of Fig. 4 were fitted with the following equation:

$$\overline{\Delta A}(\text{pH}) = \frac{\overline{\Delta A}_{\max}}{2} \frac{\sinh(1.15n(pK_{app/tr} - pK_{app/in}))}{\cosh(1.15n(\text{pH} - pK_{app/tr})) \cosh(1.15n(\text{pH} - pK_{app/in}))} \quad (4)$$

This equation was obtained in a straightforward way without approximations as the difference between two titration curves (defined in Eqn. 1) with the same amplitude $\overline{\Delta A}_{\max}$ and pK 's of $pK_{app/in}$ and $pK_{app/tr}$, respectively. For the same sample at 150 mM KCl, the apparent pK in the initial state ($pK_{app/in}$) is 6.72 ($n = 0.9$; for further details on the titration of V101C-AF in the dark see [4]). The fit results in $pK_{app/tr} = 6.90$ and $n = 0.95$. If n is constrained to 0.9, its value in the initial state, the fitted $pK_{app/tr}$ is only slightly larger (6.94). The pK -shift is thus 0.18 pH-unit. We obtain the surface potential in the transient state using Eqn. 2 with $pK_{app/tr} = 6.90$ and $pK_t = 6.31$. The latter value for the dark state was obtained for this sample as described [4]. The transient surface charge density was then obtained from Eqn. 3. We find that the surface charge at position

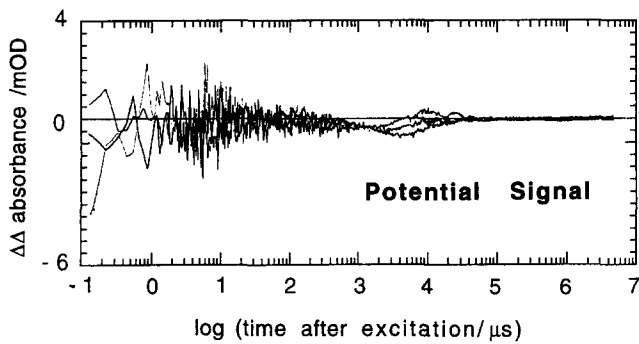


Fig. 6. Kinetics of the transient potential change at position 130 on the extracellular side for various pH-values (6.2, 6.5 and 7.2). Difference between the transient light-induced absorbance changes at 490nm of V130C and V130C-AF in 0.1% CHAPS, 0.0025% DMPC, 150 mM KCl, and 10 mM MOPS at 22°C. The logarithmic time scale is from 10^{-1} to 10^7 μ s.

101 on the cytoplasmic surface becomes transiently more negative by 0.80 elementary charge per bR. We cannot exclude an alternative explanation that the observed transient pK increase is due to a transient decrease in the dielectric constant (ϵ) of the environment of the dye [12]. In fact, experiments with fluorescein in solvents of different dielectric constants show that its pK increases by 0.7 pH-unit when ϵ decreases from 78 to 50 (data not shown). A change in the dielectric constant may be induced by a conformational change which brings the label into a more hydrophobic environment. Indeed diffraction data suggest that structural changes occur in the cytoplasmic half of bR in the M- and N-intermediates [13,14]. Recent time-resolved EPR signals on the ms time scale observed with a spin label bound to V101C were interpreted as being due to structural changes in the N- and/or O-intermediates [15]. We believe however, that the interpretation of the pK-shift as being due to a surface charge change is more likely, based on the following kinetic evidence. The time dependence of the M-intermediate and of the surface potential change detected at position 101 are compared in Fig. 5. At pH 7.3 the rise and decay times of the potential signal (2.6 ms; 60.5 ms) seem to be correlated with the two main components in the decay of M (arrows at 1.5 ms and 63.9 ms). At the other pH-values the correlation also holds. The 1.5 ms component in the M-decay of V101C-AF is most likely due to the M-to-N/O transition, in which the Schiff base is reprotonated from aspartate-96 [2,3]. The 63.9 ms component is probably due to the decay of N and O which are coupled to the M-decay by back reactions [16]. This is supported by photocycle measurements at 650 nm (data not shown), which indicate that O returns to the initial state with a decay time of 61.7 ms. Position 101 is five amino acids residues away from aspartate-96 in helix C, just above it at the cytoplasmic surface (Fig. 1). It is thus plausible that the observed pK-increase of the dye, corresponding to a change of about one negative charge per bR, is due to the transient deprotonation of aspartate-96. This interpretation is supported by recent measurements of the proton uptake kinetics as detected with fluorescein in the same

position [5]. The proton uptake time of 45 ms [5], obtained under the same experimental conditions, correlates well with the 60.5 ms decay time of the potential signal.

With fluorescein bound to position 130 on the extracellular surface no transient pK-changes were detectable in the same pH-range with a sample of the same optical density and similar label stoichiometry as used for V101C (Fig. 6). The traces shown in Fig. 6 are for pH-values close to the initial apparent pK at this position ($\text{pK}_{\text{app/in}} = 7.08$ at 150 mM KCl [4]). The photocycle of V130C-AF is not perturbed with respect to that of the unlabeled mutant and wild type. With fluorescein bound to lysine-129 on the extracellular surface of purple membranes, a transient potential change was observed with rise and decay times of 4.4 and 11.8 ms, respectively, at pH 7.5 and 150 mM KCl [10]. Our results for the adjacent position 130 are not in agreement. Since proton uptake occurs on the cytoplasmic side of the membrane, it seems more likely that a transient pK-shift on the ms time scale (due to a charge density change or a conformational change) should be sensed by a dye on that surface and not on the opposite surface.

Acknowledgements: This research was supported by grants from the Deutsche Forschungsgemeinschaft (Sfb312-B1) and from the BMFT (03-HE3FUB) to M.P.H. and by Grant AI 11479-18 from the National Institutes of Health to H.G.K.

References

- [1] Braiman, M.S., Mogi, T., Marti, T., Stern, L.J., Khorana, H.G. and Rothschild, K.J. (1988) *Biochemistry* 27, 8516–8520.
- [2] Holz, M., Drachev, L.A., Mogi, T., Otto, H., Kaulen, A.D., Heyn, M.P., Skulachev, V.P. and Khorana, H.G. (1989) *Proc. Natl. Acad. Sci. USA* 86, 2167–2171.
- [3] Gerwert, K., Souvignier, G. and Hess, B. (1990) *Proc. Natl. Acad. Sci. USA* 87, 9774–9778.
- [4] Alexiev, U., Marti, T., Heyn, M.P., Khorana, H.G. and Scherrer, P. (1994) *Biochemistry* 33, 298–306.
- [5] Scherrer, P., Alexiev, U., Marti, T., Khorana, H.G. and Heyn, M.P. (1994) *Biochemistry* 33, 13684–13692.
- [6] Alexiev, U., Marti, T., Heyn, M.P., Khorana, H.G. and Scherrer, P. (1994) *Biochemistry* 33, 13693–13699.
- [7] Carmeli, C., Quintanilha, A.T. and Packer, L. (1980) *Proc. Natl. Acad. Sci. USA* 77, 4707–4711.
- [8] Tokutomi, S., Iwasa, T., Yoshizawa, T. and Ohnishi, S.-I. (1981) *Photochem. Photobiol.* 33, 467–474.
- [9] Carmeli, C. and Gutman, M. (1982) *FEBS Lett.* 141, 88–92.
- [10] Heberle, J. and Dencher, N.A. (1992) *Proc. Natl. Acad. Sci. USA* 89, 5996–6000.
- [11] Marti, T., Rösselet, S.J., Otto, H., Heyn, M.P. and Khorana, H.G. (1991) *J. Biol. Chem.* 266, 18674–18683.
- [12] Fernandez, M.S. and Fromherz, P. (1977) *J. Phys. Chem.* 81, 1755–1761.
- [13] Subramaniam, S., Gerstein, M., Oesterhelt, D. and Henderson, R. (1993) *EMBO J.* 12, 1–8.
- [14] Vonck, J., Han, B.-G., Burkard, F., Perkins, G.A. and Glaeser, R.M. (1994) *Biophys. J.* 67, 1173–1178.
- [15] Steinhoff, H.-J., Mollaaghbababa, R., Altenbach, C., Hideg, K., Krebs, M.P., Khorana, H.G. and Hubbell, W.L. (1994) *Science* 266, 105–107.
- [16] Otto, H., Marti, T., Holz, M., Mogi, T., Lindau, M., Khorana, H.G. and Heyn, M.P. (1989) *Proc. Natl. Acad. Sci. USA* 86, 9228–9232.